ORIGINAL

Effects of molecular weight of urea–formaldehyde resins on wettability and adhesion at wood surface, interphase, and plywood

Minjeong Kim[1] · **Byung-Dae Park**[1]

Abstract

Various factors, such as molecular weight (MW), reactivity, wettability, surface roughness, surface adhesion, interphase adhesion, and cohesion of adhesives, affect the adhesion strength of urea–formaldehyde (UF) resins when bonding wood. This study was conducted to understand the MW effects of UF resins on wettability and adhesion at wood surface, interphase, and plywood. UF resins with two formaldehyde/urea (F/U) molar ratios (1.0 and 1.6) and three MW levels such as low-MW (L-MW), middle-MW (M-MW), and high-MW (H-MW) were evaluated for their wettability and adhesion. As the MW increases, the surface tension of 1.0 UF resins slightly increased, while that of 1.6 UF resins slightly decreased. The contact angle of UF resins on earlywood and latewood either from sapwood or heartwood (Radiata pine: *Pinus radiata* D. Don) before and after the extractive removal was dependent on the wood surface roughness rather than on the MWs of resins, showing a weak negative linear relationship with the surface roughness. The maximum surface adhesion force of 1.0 UF resins was greater at latewood than earlywood from sapwood before the extraction, but it decreased after the extractive removal. 1.0 UF resins showed the highest interphase adhesion at H-MW level, whereas 1.6 UF resins gave the strongest interphase adhesion at M-MW level although 1.6 UF resins had greater interphase adhesion than those of 1.0 UF resins for sapwood and heartwood. However, tensile shear strength of plywood did not proportionately relate to the wettability, surface adhesion, and interphase adhesion of UF resins. These results suggest that the MW, wettability, and surface adhesion of UF resins are indirectly related to interphase adhesion and adhesion strength in wood bonding.

✉ Byung-Dae Park
byungdae@knu.ac.kr

1   Department of Wood and Paper Science, Kyungpook National University, Daegu 41566, Republic of Korea

Introduction

UF resins are considered as one of the major adhesives for the production of wood-based composite panels, such as plywood, particle boards, and medium-density fiberboards, because of their clear color, fast curing, and low cost (Dunky 1998; Park et al. 2006; Yang et al. 2010). The performance of an adhesive in wood-based products depends on three major factors: adhesive properties (e.g., viscosity, molecular weight, and reactivity), wood parameters (e.g., wood species, surface roughness, extractives, and morphology), and processing factors (time and temperature for cold or hot pressing, etc.). In wood adhesion, the wetting, flow, penetration, and curing of adhesives at wood surface could experience some complicated physical and chemical processes. Substantial literature has studied the mechanical, physical, and chemical properties of resin adhesives for wood adhesion (Myers 1984; Dunky 1998; Park et al. 2006; Que et al. 2007; Gao et al. 2008; Alam et al. 2012; Jeong & Park 2019b). However, wood is a heterogeneous material composed of cellulose, hemicellulose, lignin, and extractives with different chemical properties, and anisotropic material with different physical properties depending on the directions (longitudinal, tangential, and radial). These parameters make wood adhesion complex processes (Merela and Čufar 2013; Pang and Herritsch 2005; Lloyd 1978; Belt et al. 2021). When the resins adhere to wood, various initial phenomena involve the wetting, spreading, and attaching of resins to the wood surface (Collett 1972; Berg 1993). In particular, "wetting" on wood surfaces is one of the signs of resin bonding. An equilibrium contact angle is obtained on the surface when the adhesion of adhesive is balanced with the solid surface by surface tension (Whitesides et al. 1991). The wetting process includes: (1) an interfacial adhesion at the surface, (2) adhesive spreading that occurs when a liquid flows over a solid surface, and (3) penetration of a liquid deep into a porous solid (Patton, 1970). Therefore, wettability is inextricably linked to the adhesion between the resin and wood (Matuana et al. 1998). Thus, it is apparent that good wetting is an important prerequisite process for establishing proper interfacial bonding and strong adhesion (Baier et al. 1968; Shi and Gardner 2001; Shupe et al. 2001; Xu et al. 2012; Petrič and Oven 2015). After wetting, actions of resins on the wood surface such as spreading, penetration, and adhesion follow.

In most studies, it is very common to evaluate the wettability using a static contact angle which is formed at an equilibrium on the solid–liquid interface because of its accessibility and simplicity (Hse 1972b; Sun et al. 2017; Wibowo and Park 2021b). In general, a decrease in contact angle (θ), which is a sign of the affinity for a solid in interfacial adhesion, leads to improved wettability (Freeman 1959; Collett 1972; Kamke and Lee 2007). Moreover, it is possible to measure not only the contact angle but also other variables to evaluate the wettability such as surface tension, surface energy, surface adhesion, and work of adhesion. For example, it is demonstrated that the contact angle of polymeric MDI resins is lower than that of MUF resins because of distinct polar components, regardless of wood species (Rathke and Sinn 2013).

In general, the contact angle, a measure of wettability, is established by the surface tension induced by the molecules attraction between two different materials

and expressed by Young's equation (Eq. 1) (Patton 1970). The contact angle is formed at an equilibrium of the surface energy (γ_L) of the liquid, the interfacial energy (γ_{SL}) between the solid and the liquid, and the surface energy (γ_S) of the solid substrate (Wang et al. 2015; Shin et al. 2018).

$$\gamma_S - \gamma_{SL} = \gamma_L \cos\theta \qquad (1)$$

The contact angle of a droplet depends on the surface properties such as roughness, cavities, permeability, or chemical properties. If the surface has a good wetting, the spreading is improved and leads to enhanced interfacial adhesion, which reflects adhesion and adhesive penetration into wood tissues. When the adhesive properly spreads, the physically rough and porous structures of heterogeneous wood surface enhance the interfacial contact area with the resin, resulting in an improved entanglement which actually facilitates mechanical bonding (Amorim et al. 2013; Rezaee Niaraki and Krause 2020; Alade et al. 2022). Of course, the contact angle between wood and liquid depends on the characteristics of a surface such as roughness and porosity. A study demonstrated that rougher earlywood surfaces of spruce and pine wood had lower apparent contact angle (Scheikl and Dunky 1998). Similarly, an increase in the surface roughness by sanding resulted in higher surface energies up to a maximum, followed by a decrease (Sinn et al. 2004). Therefore, the physico-chemical characteristics of the resin interact with the properties of the wood substrate in relation to the bonding process (Hse 1972a).

In addition, numerous studies have shown that hydrophobic characteristics and content of extractives had a detrimental impact on the wettability of resins to wood (Chen 1970; Hse and Kuo 1988; Nussbaum and Sterley 2002; Roffael 2016). As a result of the accumulation of extractives, heartwood has a substantially higher content of extractives and increases its density greater than sapwood (Wilkes 1984; Singleton et al. 2003; Cherelli et al. 2018). The extractives influence the physico-chemical properties of the wood substrate and the wettability of heartwood (Bergström et al. 1999; Zhang et al. 2004; Matsushita et al. 2012; Metsä-Kortelainen and Viitanen 2012; Belt et al. 2017; Celedon and Bohlmann 2018).

By contrast, some parameters of UF resins such as formaldehyde/urea (F/U) molar ratio, viscosity, molecular weight (MW), and reactivity have a significant impact on the chemical and mechanical properties of UF resins (Pizzi et al. 2003; Park et al. 2006; Steinhof et al. 2014; Liang et al. 2018; Wang et al. 2018; Jeong and Park 2019a, b; Lubis and Park 2020; Wibowo et al. 2020b; Wibowo and Park 2021a). The MW, chemical structure, and morphology of low molar ratio UF resins significantly differ from those of high molar ratio UF resins (Nuryawan et al. 2017; Wibowo et al. 2020b; Wibowo and Park 2022). Using a light microscope, they reported that higher molar ratio, MW, and viscosity resulted in an increased bondline thickness and decreased resin penetration into wood (Lubis and Park 2020; Wibowo et al. 2020a). Moreover, 1.6 UF resins contain longer branched molecular chains and higher MW than those of 1.0 molar ratio UF resins (Wibowo and Park, 2021a). Because the 1.6 UF resins have a branched structure with high molecular weight, they possess greater reactivity (shorter gelation time), stronger interaction with cellulose, higher maximum surface adhesion, and

work of adhesion values than those of 1.0 UF resins, indicating a relationship between the MW and wettability, or adhesion of UF resins (Wibowo and Park, 2021b).

Although wood is highly porous, resins should remain in the bondline because excessive penetration results in a starved glue line. Higher molar mass molecules of UF resins prevent a uniform distribution over a wood surface and remain on the wood surface, resulting in a delayed resin penetration (Scheikl and Dunky 1998). However, small molecules in the resin facilitate the resin penetration and cause an over-penetration, resulting in starved bondline (Gavrilovic-Grmusa et al. 2012; Jeong and Park 2019a). The viscosity also plays an important role in the bondline thickness and bond strength of plywood (Gavrilović-Grmuša et al. 2010a; b; Gavrilovic-Grmusa et al. 2012; Hong and Park 2017).

However, there is only limited literature seeking a correlation of the MW of UF resins with their wettability, surface adhesion, interphase adhesion, and adhesion strength, even though substantial research has been done on the chemistry and structure of UF resins (Pizzi et al. 2003; Park et al. 2006; Jeong and Park 2019a, b; Lubis and Park 2020; Wibowo et al. 2020b; Wibowo and Park 2021a). Therefore, the purpose of this study is to assess the influence of the MW of UF resins at different molar ratios on their wettability, surface adhesion, interphase adhesion and adhesion strength of plywood. To achieve the purpose, this study adopted a systematic approach as shown in Fig. 1. In other words, six UF resins at two molar ratios and three MW levels were synthesized and characterized for their MW, surface tension, and contact angle on the wood surface. The wood surface properties such as surface roughness and morphology before and after the removal of extractives were measured. For the first time, the maximum surface adhesion force of UF resins on earlywood and latewood either from sapwood or heartwood before and after the extraction was also determined. Moreover, their adhesion in interphase and plywood was measured to relate to their wettability and surface adhesion force.
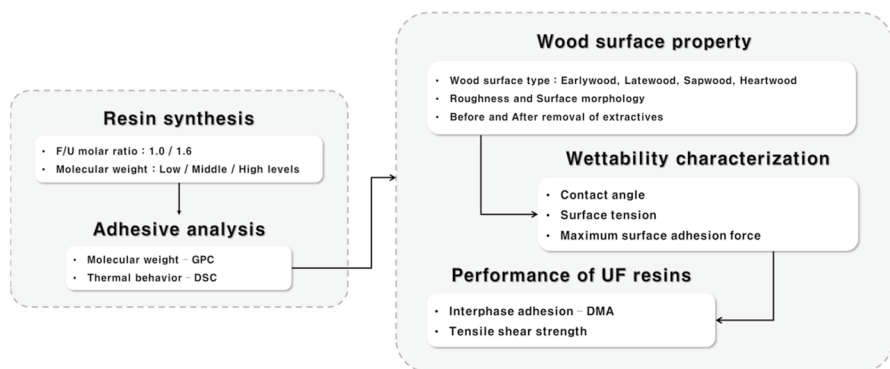
Fig. 1 Schematic diagram of the experimental work in this study

Materials and methods

Materials

Pure urea (99 wt%) and formalin (37 wt%) were purchased from Daejung Chemicals and Metals, Co., Ltd., Siheung-si, South Korea. Aqueous solutions of formic acid (20 wt%), NaOH (93 wt%), and NH_4Cl (99%) were purchased from Duksan Pure Chemicals Co., Ltd., Seoul, South Korea. HPLC-grade dimethylformamide (DMF, 99%) and dimethyl sulfoxide (DMSO, 99.9%) that were used as a mobile phase for gel permeation chromatography (GPC) were obtained from Fisher Scientific, Hampton, NH, USA, and Duksan Pure Chemicals Co., Ltd., Seoul, South Korea, respectively. Aqueous solutions of formic acid (20 wt%) and NaOH (20 wt%) were used to adjust the pH of UF resins during synthesis.

As shown in Fig. 2, earlywood and latewood specimens either from sapwood or heartwood from commercially available wood films ($43 \times 14 \times 0.15$ mm thick) of radiata pine (*Pinus radiata* D. Don) were used for the measurement of contact angle, surface roughness, maximum surface adhesion force, and interphase adhesion. Wood veneers (2 mm thick) from the same wood species were also used for plywood preparation.

Methods

Synthesis of UF resins

A three-step (alkaline–acid–alkaline) procedure was used to synthesize UF resins as previously reported by Wibowo et al. (2020a, b). Formaldehyde solution was added into a four-necked glass reactor, adjusted to pH 8.0 using sodium hydroxide (NaOH, 20 wt%), and then heated to 40 °C. Subsequently, urea was added into the reactor to give an initial formaldehyde/urea (F/U) molar ratio of 2.0. The blend was then heated to 90 °C, and the pH was maintained at 8.0 for 1 h to allow the addition reaction to proceed. Subsequently, the temperature and pH were adjusted to 80 °C and 4.6, respectively, to accelerate the condensation reaction. The molecular weight (MW) of UF resins with 1.0 and 1.6 F/U molar ratio (denoted as 1.0 UF resins and 1.6 UF resins, respectively) was controlled by adjusting the target viscosity of UF resins during the acid condensation reaction, using a bubble viscometer (VG 900, Gardener-Holdt, Columbia, SC, USA). Three target viscosity scales of "D–E," "J–K," and "S–T" were selected to obtain low MW (L-MW), medium MW (M-MW), and high MW (H-MW) level of UF resins at two molar ratios. Thereafter, the reaction was terminated at the target viscosity level, and the pH was adjusted back to alkaline (8.0–8.2). In addition, a calculated amount of the 2nd urea was added to obtain the molar ratio of 1.0 or 1.6, and the temperature was maintained at 60 °C for 20 min. Finally, the UF resins were cooled to 25 °C, and the pH was adjusted to ~ 8.2. The UF resins prepared were stored at room temperature prior to analysis.
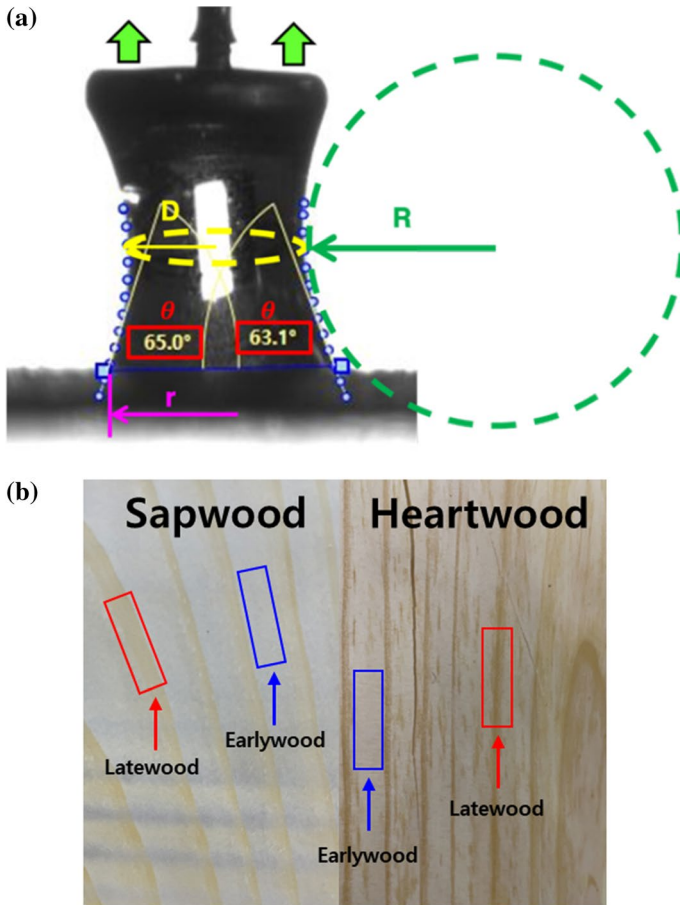
Fig. 2 Schematic diagram of **a** a UF resin droplet on a wood film surface for maximum surface adhesion force measurement at the receding stage with the contact angle (θ), droplet base radius (r), and principal radii (D and R) of the droplet, and **b** image of earlywood and latewood from sapwood or heartwood for the maximum surface adhesion force

Properties of UF resins

The viscosity of the UF resins (five resins for each of the two molar ratios) was measured on a cone–plate viscometer (DV-II+, Brookfield, Middleboro, MA, USA) using spindle no. 82 (ISO 2555, 1989) at 25 °C and 60 rpm. The non-volatile resin solids content of each resin was determined by measuring the mass of resin before and after drying in an oven for 3 h at 105 °C. For the gelation time measurement, 3% NH$_4$Cl (added as 20 wt% solution) based on the resin solids content was added to UF resins. The gelation time of UF resins prepared was measured with a gel time meter (22A Gel Time Meter, Sunshine Instruments, Vernon Hills, IL, USA) at 100 °C boiling water.

MW measurement of UF resins

A gel permeation chromatography (GPC) system (YL9100, Young Lin Instrument Co., Ltd., Hwaseong, Korea) equipped with a refractive index detector was used to measure the apparent MWs of UF resins with different molar ratios and viscosities according to the procedures reported by Jeong and Park (2019a, b) and Wibowo et al. (2020b). Prior to the measurements, 1% UF resin solution was prepared by dissolving each sample in a mixture of 10% DMSO and 90% DMF and kept in an oven at 50 °C for 3 h. Afterward, the solution was introduced into the injection loop of the GPC system after filtration through a 0.45-µm filter. The columns used were KD-801, KD-802, and KD-806 M (Shodex, Showa Denko K.K., Tokyo, Japan). Poly (ethylene glycol) with a MW between 106 and 25,200 Da (Polymer Standards Service GmbH, Mainz, Germany) was used as calibration standards. Weight-averaged molecular weight (M_W), number molecular weight (M_n), and polydispersity index (PDI) were calculated using the software YL-Clarity Version 6.1.0.130 (Young Lin Instrument Co., Ltd., Hwaseong, South Korea).

Thermal curing behavior of UF resins

A differential scanning calorimeter (DSC) (DSC 25, TA Instruments, New Castle, DE, USA) was used to analyze the curing behavior of UF resins. 3% NH_4Cl based on the non-volatile solid content was mixed to prepare a 5–6 mg sample of UF resins. Then, it was sealed in a high-pressure capsule pan to suppress the evaporation of water during DSC scanning. Each sample was scanned at a heating rate of 2.5, 5, 10, and 20 °C/min in the temperature range of 30 °C–200 °C under a flow of nitrogen gas at 50 mL/min. After scanning, all thermograms of the UF resins were analyzed using a commercial software (TRIOS software, v4.3.0, TA Instruments, New Castle, DE, USA) to obtain the peak temperature at the exothermic curve.

Surface tension measurement using Wilhelmy plate

The surface tension (σ, in milli-newton per square centimeters) of UF resins is also measured because the surface tension is one of the wettability factors of adhesives at the interface (Wålinder, 2000; Wålinder and Ström, 2001; Khan et al. 2004; Lee et al. 2007). According to the procedure in DIN 53914 (1997), the surface tension of UF resins at different molar ratios and MWs was measured using a Wilhelmy plate (10 × 19.9 × 9.2 mm, PT 11, Data Physics Instruments GmbH, Filderstadt, Germany) and a weighing system attached to a tensiometer (DCAT 25, Data Physics Instruments GmbH, Filderstadt, Germany; Nayar et al. 2014). A vessel was filled with UF resins up to a height of at least 4 mm, which served as the sample stage. A measuring Wilhelmy plate (8 mg) was immersed in the UF resins to a depth of 3–30 mm at a rate of 1 mm/s and wetted by the UF resins along the perimeter of the plate. The surface tension of UF resins can be calculated using the contact angle between plate and resin. As tension force (F_{tens}) acts tangentially to the liquid surface at the

three-phase contact line, and it can be divided into two parts (Rapp 2017): the parallel force ($F_\parallel$) to the undisturbed liquid surface and the perpendicular force ($F_\perp$) to it are expressed by Eqs. 2 and 3:

$$F_\parallel = F_{\text{tens}} \times \sin \theta_C \tag{2}$$

$$F_\perp = F_{\text{tens}} \times \cos \theta_C \tag{3}$$

where $\sin \theta_c$ and $\cos \theta_c$ are the parallel and perpendicular contact angle to the surface. At this point, the z-direction balance only measures the perpendicular part of the tension force, which coincides with the gravitational force (F_G) of the formed surface. The balance of the tensiometer measures the weight of the attached plate at the beginning of the measurement to build the Wilhelmy equation based on this theory. If the plate surface is being contacted with liquid as it moves into the liquid, the surface tension of a liquid is automatically calculated by the Wilhelmy equation as shown:

$$\sigma = \frac{F_{\text{tens}}}{L} = \frac{F_\perp}{L \cdot \cos \theta_C} = \frac{F_G}{L \cdot \cos \theta_C} \tag{4}$$

Based on Eq. (4), the surface tension (σ) as tensile force per length of the contact line can be obtained when the Wilhelmy plate is completely wet (contact angle $= 0°$).

Contact angle measurement of UF resins

The contact angles of UF resins on different types of wood surfaces (earlywood and latewood either from sapwood or heartwood) were measured using a camera system of the tensiometer according to the procedure reported by Wibowo and Park (2021a). In brief, sessile drop contact angle measurements were taken to determine the angle formed when a droplet of UF resins was deposited on the surface of different wood types. The contact angle image was taken using the camera system in 30 s after a droplet of UF resins was added on the wood surface. Afterward, the horizontal baseline on which the droplet of UF resins was being deposited was determined by drawing the droplet edges. Finally, the software automatically calculated the gradient of the tangent of the droplet edge at the point where it met the baseline and contact angle between the baseline and a gradient.

Maximum surface adhesive force measurement of UF resins on wood surface

As shown in Fig. 2, the maximum adhesion force of a droplet of UF resins with different molar ratios and MWs on different wood types was determined using the same tensiometer according to the procedure reported by Wibowo and Park (2021a). A droplet of UF resins suspended on a Du Noüy ring (RG 2, Data Physics Instruments GmbH, Filderstadt, Germany) was advanced to the respective wood surface, and then the liquid droplet was receded by pulling off the surface. A force–distance curve was automatically recorded during this procedure. The surface of a wood

sample was moved upward toward the UF resin droplet at an advancing speed of 0.5 mm/s until the wood sample surface came in contact with the surface of the droplet. After reaching the compression distance (0.1 mm), the wood film sample was receded from the droplet at the same advancing speed until the droplet was detached from the surface of the wood film sample. Preliminary investigations determined the speed based on the maximum adhesive force with the smallest standard deviation.

The interactive force between the droplet and solid surface is called the adhesion force (F). F consists of two components. The first component is the surface tension force (F_S), which is the vertical component of the liquid–gas interfacial tension along the perimeter of the triple-phase contact line, and the second component for a stretched droplet is the capillary pressure force (F_L), which is created by a curvature of the liquid due to pressure difference across the liquid–gas interface. These forces can be expressed by Eq. (5) (Sun et al. 2017; Wang et al. 2020; Wibowo and Park, 2021b):

$$F = F_S - F_L = 2\pi r\gamma \sin\theta - \pi r^2 \Delta P \tag{5}$$

where r is the base radius of a droplet that is in contact with the substrate, γ is the liquid–gas interfacial tension, θ is the contact angle, and ΔP is the pressure difference between the interior and exterior of a droplet interface known as Laplace pressure in Eq. 6:

$$\Delta P = \gamma\left(\frac{1}{D} - \frac{1}{R}\right) \tag{6}$$

where D and R are the principal radii of the droplet. This equation is based on the equilibrium and is thus only used for quasistatic conditions. Depending on whether the shape of a droplet is convex or concave, ΔP might be positive or negative. The contact angle at the maximum adhesion force (F_{max}) is the most stable contact angle (θ_{max}). As all of the stretched droplets have a concave shape, ΔP was calculated by Eq. (6). Detailed information related to this equation can be found in the literature (Butt et al. 2014; Chen et al. 2015, 2016). F_{max} was recorded at the θ_{max} identified from a typical recorded image and represented by the peak of a force–distance plot. Subsequently, the F_{max} value was calculated by Eq. (5). This experiment was repeated at least three times for each sample.

Surface roughness measurement of wood films

The surface roughness of the wood film surface (earlywood and latewood in sapwood and heartwood of radiata pine) was measured using a contact stylus surface roughness tester (HUATC SRT-6210, International Standard 4287) with a 2-µm diamond stylus, employing a cutoff length of 2.5 mm, a measuring length of 2 mm, and a speed of 1 mm/s at three replications according to the standard method (ISO 4288 1997). The surface roughness parameters were evaluated as the arithmetic mean of the sum of a roughness profile value (R_a) and the root-mean-squared value (R_q) according to Eqs. (7) and (8), respectively (ISO 4288 1997).

$$R_a = \frac{1}{N} \sum_{i=1}^{N} |Y_i| \tag{7}$$

$$R_q = \frac{1}{N} \sum_{i=1}^{N} |Y_i|. \tag{8}$$

Extractive removal of wood samples

The extractives of the wood film samples were removed by ethanol–benzene extraction according to TAPPI method (T204 cm-97, 1997). A flask containing 150 mL of ethanol–benzene mixture (1:2 *v/v*) was coupled to a Soxhlet extraction tube containing ~ 0.04 g of wood films. The extraction was done for at least six cycles per hour. After at least 24 cycles of extraction, the resulting extractive-free samples were used for wettability test.

Interphase adhesion of UF resins/wood film composites

As shown in Fig. 3, two thin wood films (radiata pine) were bonded with UF resins at different molar ratios and MWs to prepare UF resin/wood film composites at a glue spread of 125 g/m², which was an optimum level determined in a previous work (Jeong and Park 2019a). The prepared composite sample (100 mm × 8 mm × 0.15 mm) was used to measure maximum storage modulus (E'_{max}) as an interphase adhesion using dynamic mechanical analysis (DMA, Q800, TA Instruments, New Castle, DE, USA) in dual cantilever mode. DMA measures modulus and damping as a function of temperature and frequency. All samples were pre-cured in an oven at 50 °C for 20 min prior to DMA analysis. The storage modulus (E') of each sample was determined at a frequency of 1 Hz, strain level of 0.005%, and heating rate of 5 °C /min in the scanning range of 30 – 300 °C (Jeong and Park 2019b).
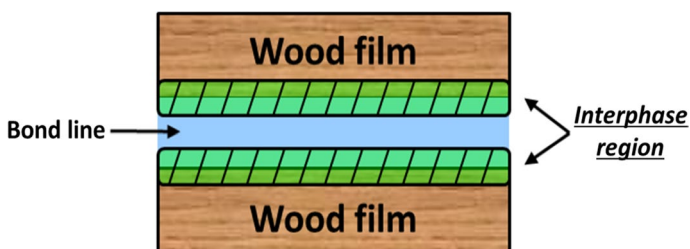
Fig. 3 Schematic diagram of UF resin/wood film composite for interphase adhesion measurement

Measurement of tensile shear strength of plywood

Three-ply plywood was prepared using wood veneers from radiata pine (*Pinus radiata* D. Don). UF resins mixed with 3% NH_4Cl on the basis of non-volatile resin solid content, and approximately 10% wheat flour based on the total mass of the UF resins were applied to the veneer surface at a glue spreading rate of 170 g/m^2 using a rubber roller. After the pre-assembled plywood was cold-pressed under a pressure of 1.4 MPa for 20 min, it was hot pressed at 120 °C for 4 min at the same pressure. Tensile shear strength (TSS) of a plywood was determined according to a standard process (KS F 3101 2020). As shown in Fig. 4, nine specimens ($25 \times 80 \times 6$ mm) were used to determine TSS at a crosshead speed of 2 mm/min using the peak load of a universal testing machine (H50KS, Hounsfield, Redhill, England). Statistical analysis was conducted using two-way ANOVA and Duncan's multiple range test.

Results and discussion

Table 1 shows the properties of 1.0 and 1.6 UF resins synthesized to have different MW levels. The MW levels of 1.0 and 1.6 UF resins were controlled by adjusting a target viscosity during the resin synthesis and expressed as low MW (L-MW), medium-MW (M-MW), and high-MW (H-MW) levels. MWs of 1.6 UF resins are greater than those of 1.0 UF resins even though the same target viscosity is used. As expected, the viscosity and MW of 1.6 UF resins are greater than those of 1.0

**Fig. 4** Schematic diagram and dimensions of TSS specimen of plywood (unit: mm)
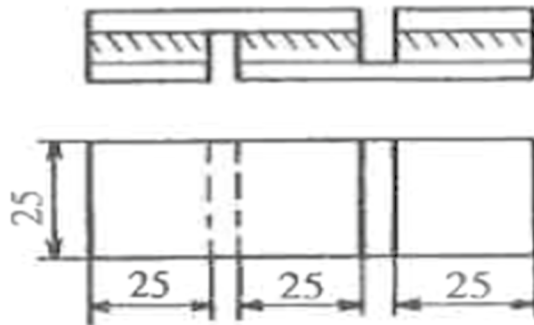
Table 1 Properties of UF resins synthesized at two F/U molar ratios and three MW levels

F/U molar ratio	M_w (g/mole)	MW level	pH	Viscosity (mPa·s)	Non-volatile solid content (wt%)	Gelation time (s)
1.0	383	L-MW	8.0	189.4	56.9	141
	527	M-MW	8.2	215.6	59.6	151
	656	H-MW	8.0	256.9	59.2	165
1.6	617	L-MW	8.1	213	52.5	55
	709	M-MW	8.3	365.6	52.7	57
	897	H-MW	8.3	663.1	53.7	54

UF resins. This is due to the higher reactivity of 1.6 UF resins than 1.0 UF resins. The non-volatile solid contents of 1.0 UF resins are higher than that of 1.6 UF resins because of a higher amount of the second urea than that of 1.0 UF resins (Pizzi 1983; Park 2007; Wang et al. 2018). Moreover, the most noticeable difference is that the gelation time of 1.6 UF resins is much shorter than those of 1.0 UF resins as reported in previous studies (Park et al. 2006; Hong and Park 2017). This is probably because 1.6 UF resins are highly branched structures with many methylene ether linkages. Thus, 1.6 UF resins became a gel in a much shorter time by forming a network structure than 1.0 UF resins that contained de-branched hydroxymethyl groups and linear structures (Wibowo et al. 2020b; Wibowo and Park 2021b).

Figure 5 shows the number average molecular weight (M_n), weight average molecular weight (M_w), and polydispersity index (PDI) of UF resins at different
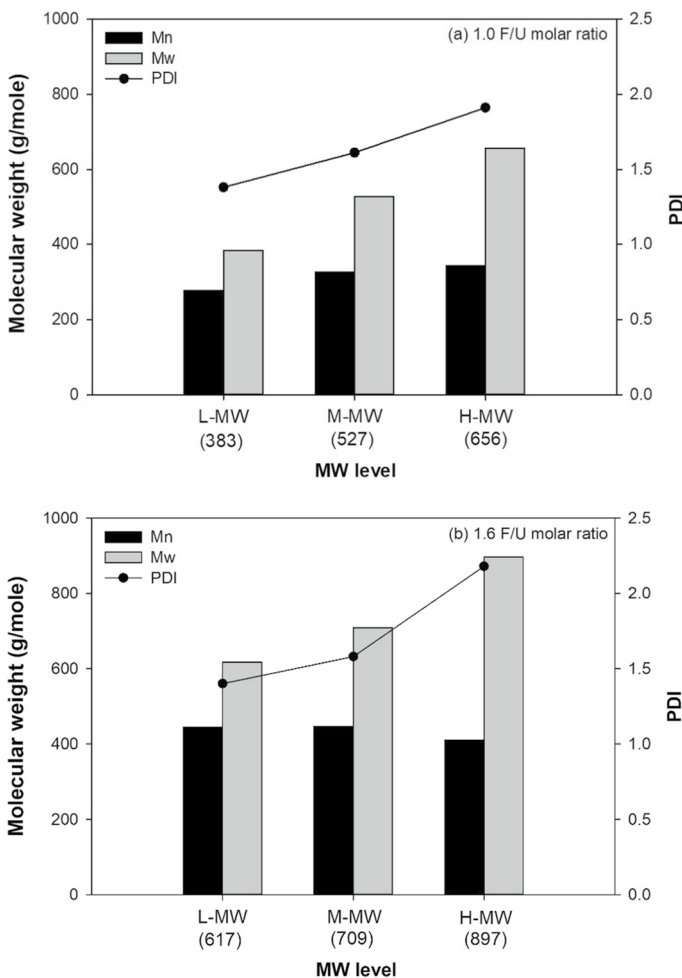

Fig. 5 M_n, M_w, and PDI of 1.0 and 1.6 UF resins at different molar ratios and MW levels; **a** 1.0 UF resins and **b** 1.6 UF resins

MW levels and molar ratios. Both 1.0 and 1.6 UF resins exhibited a similar trend in their viscosity and MW. As the viscosity increases, the MW also increases. All M_n, M_w, and PDI values of 1.6 UF resins in all viscosity scales are significantly larger than those of the 1.0 UF resins due to the branched polymer in the condensation reaction as reported in previous studies (Wibowo et al. 2020b; Wibowo and Park 2021b). 1.0 UF resins resulted in lower MW than those of 1.6 resins because the amount of the second urea decreased the degree of branching of the resins (Wang et al. 2018; Lubis and Park 2020). In addition, urea could be activated by hydroxyl ions that can react with positively charged carbons of the oxymethylene and methylene ether linkages in branched polymers so that linear polymers with a lower MW could take up a large portion of the UF resins (Wibowo and Park 2021b). The M_n and PDI of 1.0 UF resins showed a linear relationship, but this was not the case for 1.0 UF resins. An increase in the PDI values indicates that the resins have more branched molecules (Lubis and Park 2021). However, the rapidly increased PDI values and slightly decreased M_n of 1.6 UF resins with the highest molecular weight suggested that 1.6 UF resins had heterogeneous structures and highly branched molecules (Jiang et al. 2021).

Figure 6 shows changes of the peak temperature (T_p) at which the highest conversion rate occurs during the curing reaction to compare the curing behavior of UF resins with different molar ratios and MWs. All DSC thermograms of UF resins are presented in Fig. S2 in Supplementary Material. The T_p of UF resins corresponds to a maximum polycondensation reaction of the polymeric moieties between the primary amino groups and hydroxymethyl groups of the resin (Siimer et al. 2003). As expected, the T_p also increased as the heating rate increased from 2.5 °C/min to 20 °C/min, regardless of the MW level and molar ratio of UF resins. In addition, Fig. 6 shows that T_p of 1.0 UF resins is higher than that of the 1.6 UF resins, indicating that more heat is released from the maximum polycondensation reaction of the primary amino groups of unreacted urea with the hydroxymethyl groups (mono-,di-, or tri-hydroxymethyl) in 1.0 UF resins. Therefore, the resin reactivity of resin curing increased as the F/U molar ratio increased. In addition, the T_p tends to decrease as the MW increases, which is consistent with other results (Siimer et al. 2003; Park et al. 2006; Lubis and Park 2018).

Figure 7 shows the surface tension obtained from the Wilhelmy plate, depending on the molar ratio and MWs. The surface tension of 1.0 UF resins is greater than those of 1.6 UF resins even though the MWs of 1.0 UF resins are smaller than those of 1.6 UF resins. The surface tension of 1.0 UF resins is statistically different at the MW levels, while it is not the case for 1.6 UF resins (see Table S1 in Supplementary Material). This could be due to a difference in the resin solids content. In other words, a higher resin solids content of 1.0 UF resins has greater surface tension than 1.6 UF resins that have a lower resin solids content. These results show that the resin solids content of UF resins clearly influences their surface tension. The surface tension values obtained in this study are comparable to the published value of 63.0 dyn/cm for pure UF resins (Lee et al. 2007).

Figure 8 shows the surface roughness (R_a and R_q) of the earlywood and latewood either from sapwood or heartwood of the wood film. R_q values are calculated as the square of the amplitude and are more sensitive to the peaks and
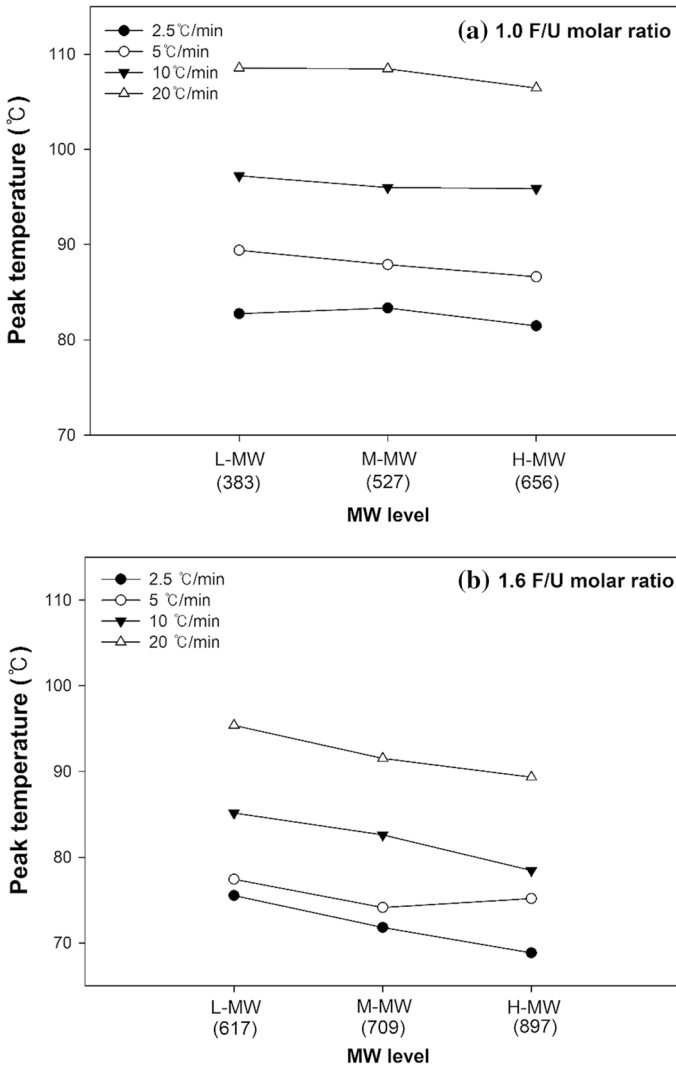
Fig. 6 Change of T_p of UF resins with **a** 1.0 and **b** 1.6 F/U molar ratios at different MW levels and heating rates

valleys of a surface. Thus, it always maintains greater values than R_a. Earlywood has higher R_a and R_q values than latewood, regardless of sapwood or heartwood, which is comparable with reported results, regardless of surface treatment (Follrich et al. 2010). However, there is no difference in the surface roughness between sapwood and heartwood.

Earlywood either from sapwood or heartwood shows greater surface roughness than latewood as the earlywood from sapwood or heartwood has larger lumens and a greater number of inter-wall cracks than latewood (see Figs. S3 and S4 in
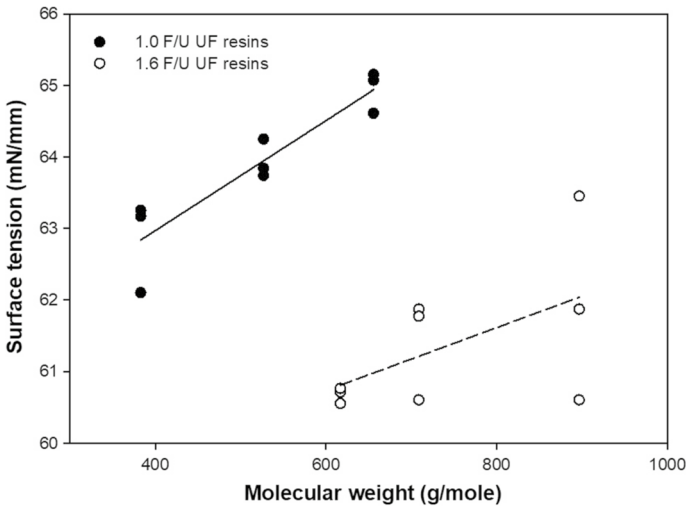
Fig. 7 Surface tension of 1.0 and 1.6 UF resins with different MW levels using Wilhelmy plate method. *The statistical data related to this figure are presented in the supplementary information (Table S1)

Supplementary Material). In addition, the surface morphology between sapwood and heartwood is not much different because there is no significant difference in the microstructures between sapwood and heartwood. The difference in the mesopore structures of the earlywood and latewood from sapwood could be related to structural features of the cell wall. The density of latewood is 2.3 times higher than that of earlywood from sapwood because of differences in the cell wall thickness. However, the surface roughness of heartwood may not be affected because a similar amount of micropores and mesopores exists in earlywood and latewood, which are highly affected by extractives (Plomion et al. 2001; Dehon et al. 2002; Yin et al. 2015).
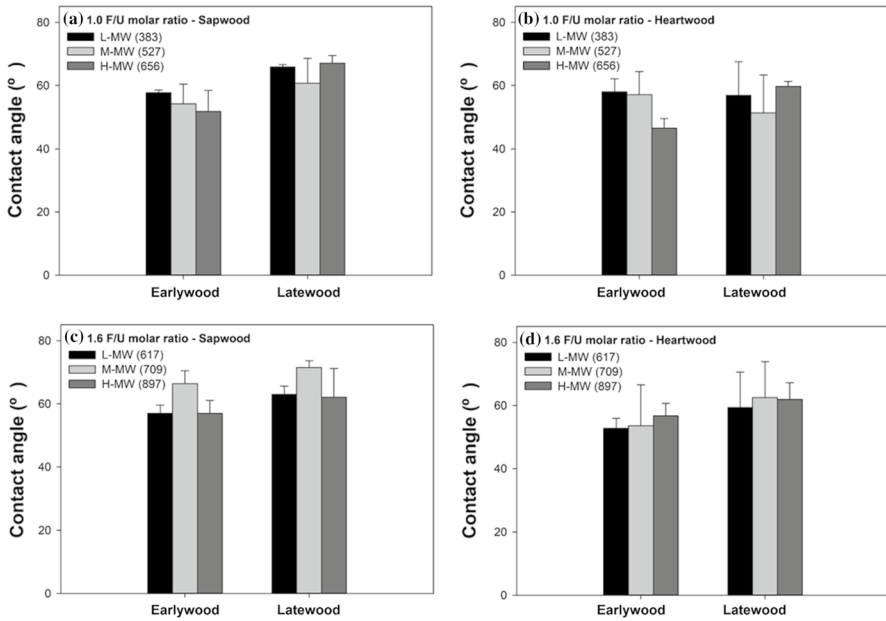
The contact angle of 1.0 and 1.6 UF resins with L-, M-, and H-MW levels on the surface of earlywood and latewood either from sapwood or heartwood before the extractive removal is presented in Fig. 9. As expected, the contact angles of 1.0 and 1.6 UF resins on the earlywood from sapwood are relatively lower than those of UF resins on latewood. This could be due to the large lumens exposed in earlywood and an increase in the surface roughness, indicating that wood type affects their wettability (Hse 1972b; Shupe et al. 1998). In addition, the contact angle on heartwood is smaller than those on sapwood because heartwood in dark color has a lower permeability and significantly higher extractive than sapwood. 1.0 UF resins with the highest MW have the largest contact angle on earlywood. However, 1.0 UF resins with M-MW have the largest contact angles on latewood (both from sapwood and heartwood), indicating that UF resins with M-MW have greater wettability on latewood in contrast to the earlywood because the surface roughness of earlywood produces topographic heterogeneity on wood surfaces. In addition, the contact angle could be related to the resin penetration into wood because a rougher surface with porous structures enhances capillary forces allowing for small adhesive molecules to penetrate into the pores in a greater depth (Cheng and Sun 2006).
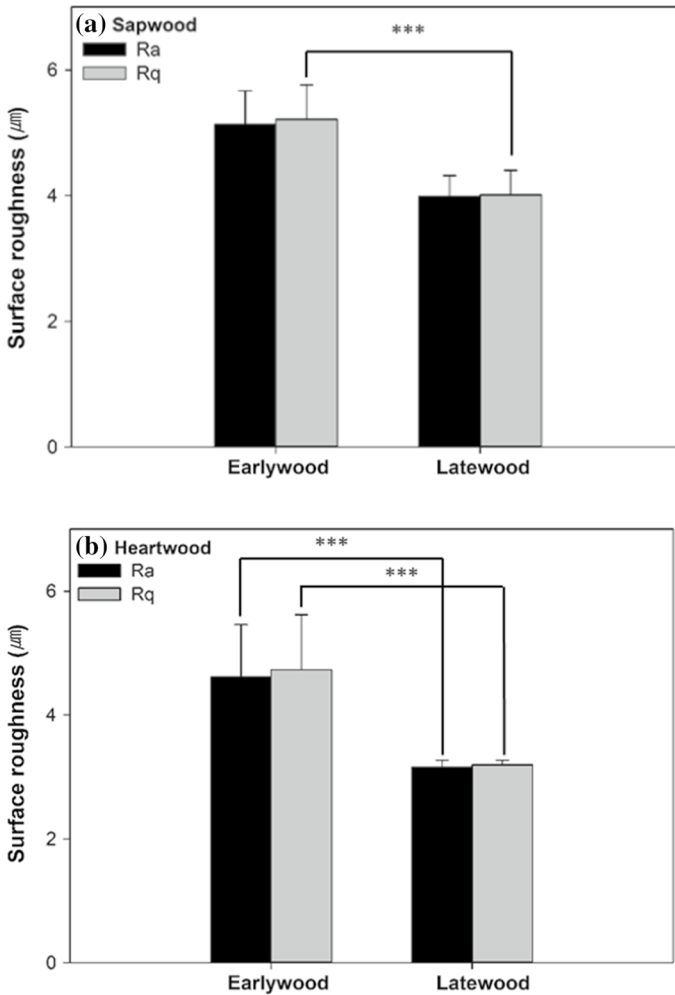
Fig. 8 R_a and R_q values of different wood types: **a** earlywood and latewood from sapwood, **b** earlywood and latewood from heartwood. The symbol (***) shows that they are significantly different at a *p*-value of 0.01 by *T* test

The maximum surface adhesion force is the adhesion force between a resin droplet and wood surface at the peak of the force–distance curves in four steps (Sun et al. 2017; Wibowo and Park 2021b). A typical force-distance curve of UF resins on the wood surface is presented in Fig. S1 in Supplementary Material. Figure 10 shows the maximum surface adhesion force of 1.0 and 1.6 UF resins with L−, M−, and H-MW on the surface of different wood types. Regardless of wood types, 1.0 UF resins showed greater maximum surface adhesion force than 1.6 UF resins. This could be partially responsible for the high resin solids content of 1.0 UF resins. In other words, a greater polymer fraction of 1.0 UF resin per unit volume could provide more adhesion to the wood surface than 1.6 UF resins did because 1.6 UF

Fig. 9 Contact angles of 1.0 and 1.6 UF resins with different MW levels on different wood types; **a** and **b** 1.0 UF resins on the earlywood and latewood from sapwood and heartwood, respectively; **c** and **d** 1.6 UF resins on the earlywood and latewood from sapwood and heartwood, respectively
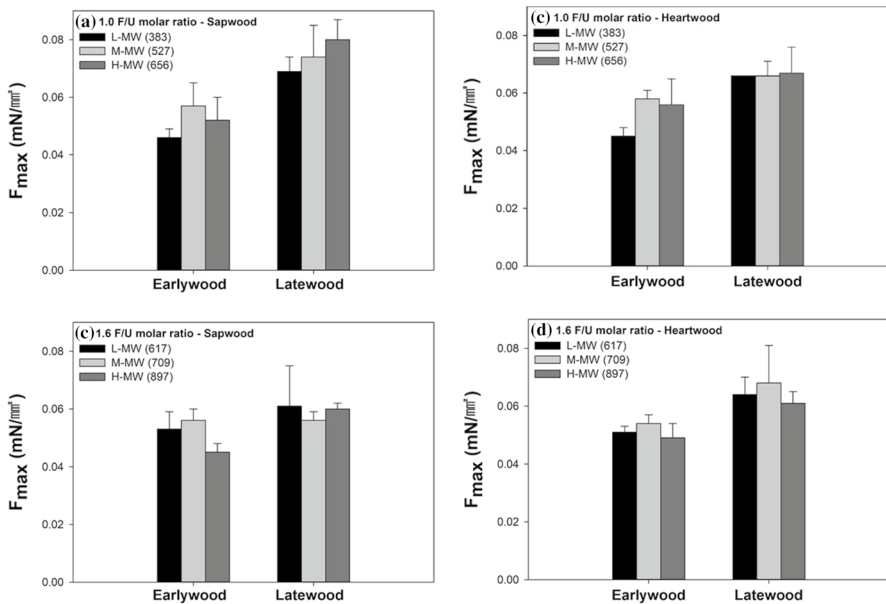

Fig. 10 Maximum surface adhesion forces of 1.0 and 1.6 UF resins with different MW levels on different wood types; **a** and **b** 1.0 UF resins on the earlywood and latewood from sapwood and heartwood, respectively; **c** and **d** 1.6 UF resins on the earlywood and latewood from sapwood and heartwood, respectively

resins had lower resin solids content. Moreover, the polymeric species of high MW could have resulted in strong cohesion as the polymer chain becomes longer due to an increase in molecular entanglements (Myers 1999; Wibowo and Park 2021a).

In addition, 1.0 UF resins showed the strongest adhesion force on the latewood from sapwood, while the surface adhesion force of earlywood from sapwood was smaller than those of latewood surface. This could be due to a greater surface roughness of the earlywood than that of latewood. The maximum surface adhesion force of 1.0 UF resins increased for the sapwood only as the MW level of UF resins increased (Fig. 10a). In general, high surface roughness reduces the effective contact area of the surface and maximum pull-off traction, leading to a low adhesion at the surface (Henry et al. 2012; Joe et al. 2020; Wibowo and Park 2021a). However, it is contrasting to the reported results that a greater amount of extractives comprising small, non-wettable organic molecules in the latewood of Southern pine explains the higher contact angle of the UF resins on latewood than on earlywood (Šernek et al. 2004). However, 1.6 UF resins did not show a clear trend in the surface adhesion force on earlywood and latewood from sapwood or heartwood.

The extractives in radiata pine are more abundant in heartwood than sapwood, and their quantity and composition are dependent on the percentage of inherent heartwood and the age of the wood (Hillis 1972). Moreover, resin acids made up a considerable amount of the total extractives in the heartwood of radiata pine, accounting for 70–80% of the total extractives, while sapwood resin acids made up 40% (Hillis 1962). More specifically, mature and juvenile (sapwood and heartwood) 19–28-year-old radiata pine have 0.2% and 0.6% of extractives, respectively (Hillis 1962). Latewood from heartwood contains more extractives than earlywood because of the high amount of resin acids due to concentration caused by the formation of heartwood for a long time (Lloyd, 1978). In addition, the toxic compounds of extractives increased the wood density. Thus, the fine texture of denser wood reduced wettability (Santoni and Pizzo 2011). Moreover, previous studies have shown that sapwood is more wettable than heartwood of Douglas fir and Southern pine, which both contain non-wettable extractives (Shi and Gardner 2001). Wood species with high extractive content, such as sessile oak and spruce, have higher contact angles than those with low extractive content (Timell 1986). Therefore, it is possible to compare the effect of the presence/absence of extractives on the surface properties of wood and its wettability.

To understand the effect of extractives on wettability, extractives of wood were removed by extraction with an ethanol–benzene mixture. Figure 11 shows the surface roughness of the earlywood and latewood from heartwood or sapwood before and after the extractive removal. The surface roughness of the earlywood from sapwood or heartwood increased after the extraction, whereas that of latewood decreased slightly after the extraction. As presented in Figs. S3 and S4 in Supplementary Material, the surface roughness of earlywood qualitatively shows larger cavities after the extraction, which could be responsible for increased surface roughness (Santoso et al. 2019). However, the surface roughness of heartwood is smaller than that of earlywood from sapwood or heartwood, which could be due to an improved homogeneity of the surface after the extractive removal.
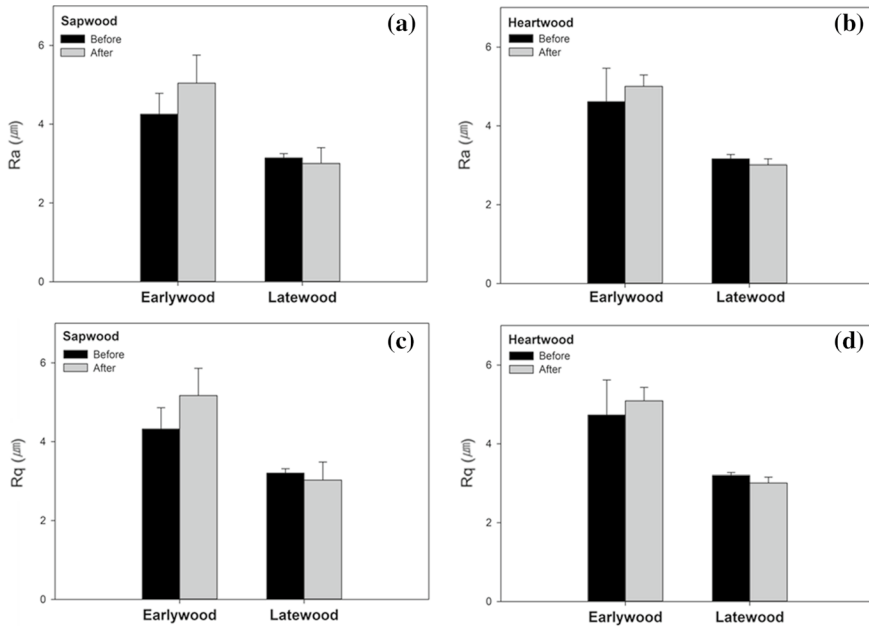
Fig. 11 R_a and R_q values of wood types before and after the removal of extractives: **a** and **b** R_a of earlywood and latewood from sapwood and heartwood, respectively; **c** and **d** R_q of earlywood and latewood from sapwood and heartwood, respectively

In addition, Figs. S3 and S4 in Supplementary Material show SEM images of the earlywood and latewood from sapwood or heartwood before and after the extraction. Even though it is a qualitative comparison, Fig. S4 illustrates that the earlywood images from sapwood or heartwood show more cavities after the extraction than before. However, the SEM images of the earlywood and latewood from heartwood look not much different to before and after the extraction, which results in a slight change in their surface roughness. A more detailed chemical analysis will help to determine how the chemical composition of extractives affects wettability.

To understand the wettability of UF resins on the surface of different wood types after the extraction, the contact angle of UF resins was measured, and the results are presented in Fig. 12. After the extraction, the contact angles on earlywood from sapwood and heartwood decreased, while those of latewood increased for both wood types. Moreover, the contact angles of sapwood were relatively higher than those of heartwood, regardless of earlywood or latewood. This result is very consistent with the surface roughness of wood after the extraction. In other words, the contact angles of earlywood from sapwood or heartwood decreased as the extractive removal increased the surface roughness. This result corresponds to an improved wettability of other woods (*Subcordate alnus* and *Zelkova carpinifolia*) after the extractive extraction (Ghofrani et al. 2016). By contrast, the contact angles on latewood slightly increased after the extraction except for the latewood from heartwood with 1.6 UF resins. This could be due to the fact that the latewood has fewer cavities and lower surface roughness than earlywood. These results suggest that the
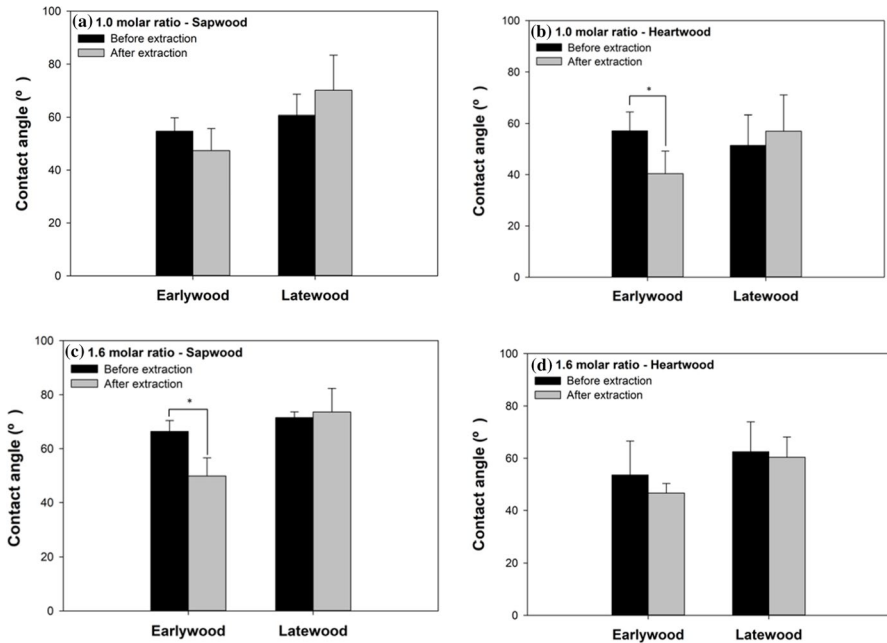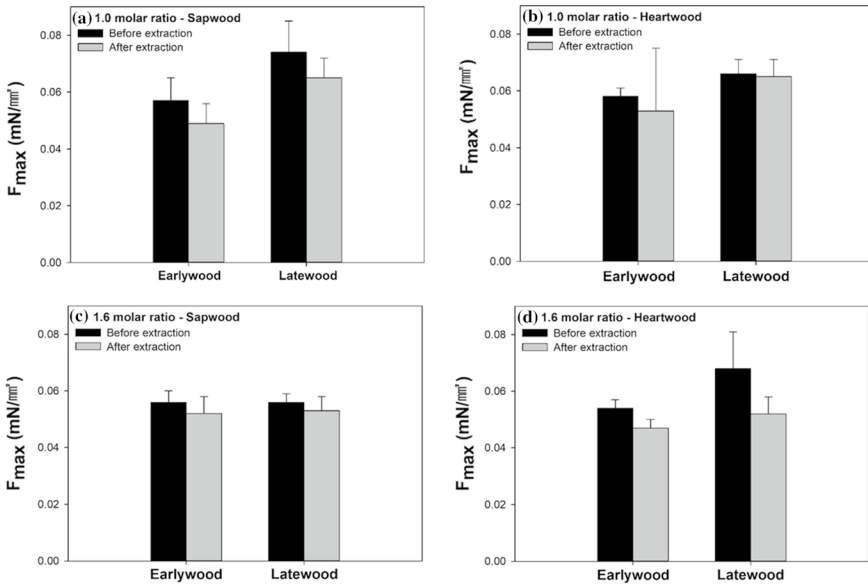
Fig. 12 Contact angles of 10 and 1.6 UF resins with M-MW on different wood types: **a** and **b** earlywood and latewood from sapwood and heartwood, respectively, for 1.0 UF resins; **c** and **d** earlywood and latewood from sapwood and heartwood, respectively, for 1.6 UF resin. *The averages are statistically different at a p value of 0.05

extractive removal in the earlywood film affects the contact angle by changing the surface roughness and chemical composition.

Figure 13 also shows the maximum surface adhesion force of UF resins with M-MW level on wood surfaces before and after the extraction. The surface adhesion force of earlywood and latewood decreased after the extraction, except for latewood from sapwood and heartwood with 1.0 UF resins. These results could be due to the fact that the extraction increased the surface roughness of earlywood, leading to lower surface adhesion force.

As discussed, it seems that the surface roughness of wood dominantly affects the contact angle and maximum surface adhesion force of UF resins on wood surfaces. Thus, a correlation between the contact angle and surface roughness (Ra values) is made and the result is presented in Fig. 14. As expected, the contact angle revealed a negative relationship with the surface roughness of wood. This result is similar to other results reported (Papp and Csiha 2017). However, the linear relationship between them is weak with a low R-square value (0.334).

In order to relate the contact angle and maximum surface adhesion force to the adhesion of UF resin in the interphase, the composites prepared by bonding two wood films of sapwood or heartwood together with UF resins were tested with DMA. Figure 15 shows the maximum storage modulus (E'_{max}), which is regarded as interphase adhesion of the UF resins/wood composites. The interphase

Fig. 13 Maximum surface adhesion force of 1.0 and 1.6 UF resins with M-MW level on different wood types before and after the extractive removal: **a** and **b** 1.0 UF resins; **c** and **d** 1.6 UF resins
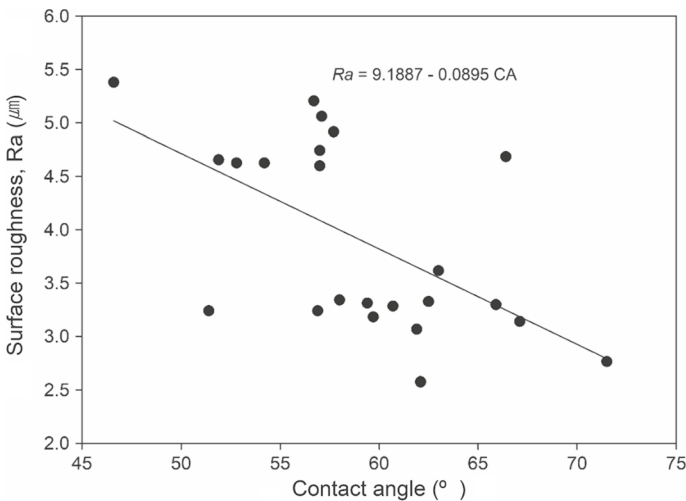
Fig. 14 Correlation between the contact angle of UF resins and surface roughness of the wood surface

adhesion of 1.0 UF resins roughly increased with an increase in the MW level, leading to the highest E'_{Max} values at H-MW level for sapwood and heartwood. As expected, the E'_{Max} of 1.6 UF resins was higher than those of 1.0 UF resins. However, the interphase adhesion of 1.6 UF resins was the highest at M-MW
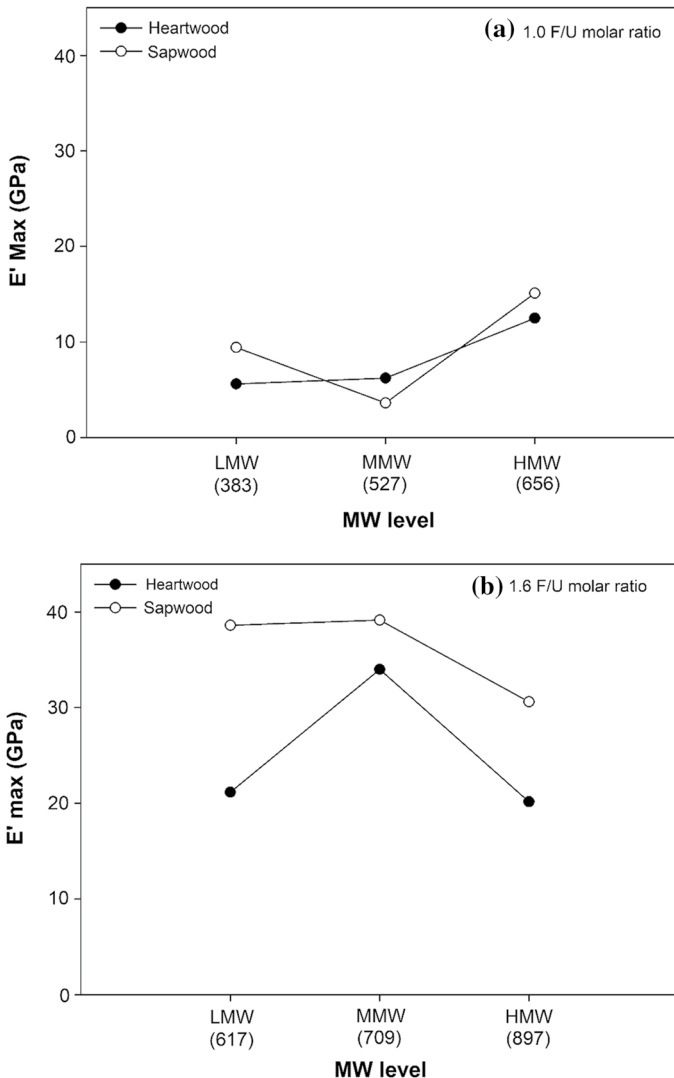
Fig. 15 E'_{Max} of UF resins with L-MW, M-MW, and H-MW on different wood types: **a** 1.0 UF resins; **b** 1.6 UF resins

level, not at H-MW level. This could be due to the fact that low MW species deeply penetrated into amorphous wood polymers, whereas high MW species mainly remained in the bondline (Laborie et al. 2006; Nuryawan et al. 2014). In general, it is well known that 1.0 UF resins comprise more linear and low MW molecules than 1.6 UF resins (Wibowo and Park, 2022). However, 1.6 UF resins had higher MW species and provide strong cohesive force but poor penetration (Jeong and Park 2017). However, it seems that the effect of sapwood and heartwood on the interphase adhesion is overwhelmed by the resin properties such as

MW, gelation time, and molecular structures. In addition, the interphase adhesion of 1.0 UF resins for the earlywood from sapwood or heartwood follows a similar trend to the surface maximum adhesion force of the same resins as shown in Fig. 10. Moreover, the interphase adhesion of 1.6 UF resins also had a similar trend to the maximum surface adhesion force as presented in Fig. 10.

Figure 16 shows tensile shear strength (TSS) results of plywood bonded with UF resins at different MW levels. According to the statistical analysis using T test, there is no significant difference for TSS values of UF resins with different MWs and F/U molar ratios (see Table S2). Moreover, the higher the MW level, the higher the tensile shear strength value, which is independent of the F/U molar ratios. UF resins with a high F/U molar ratio and a considerable quantity of formaldehyde emission (FE) have strong molecular reactivity and numerous cross-linking structures, which promote remarkable bond strength (Myers 1984; Li and Zhang 2021; Wibowo and Park 2021b). However, unlike the wettability and interface adhesion, the TSS of plywood displays a significant difference between high and low F/U molar ratio resins. This could be due to the fact that UF resins with high F/U molar ratio have higher MW than those of the UF resins with low F/U molar ratio, and they are more viscous, have a thick bondline, and penetrate poorly (Nuryawan et al. 2014). Therefore, as the UF resins with higher molar ratio are not thoroughly wetted on the surface, their contact angle is much higher than that of the UF resins with lower molar ratio.
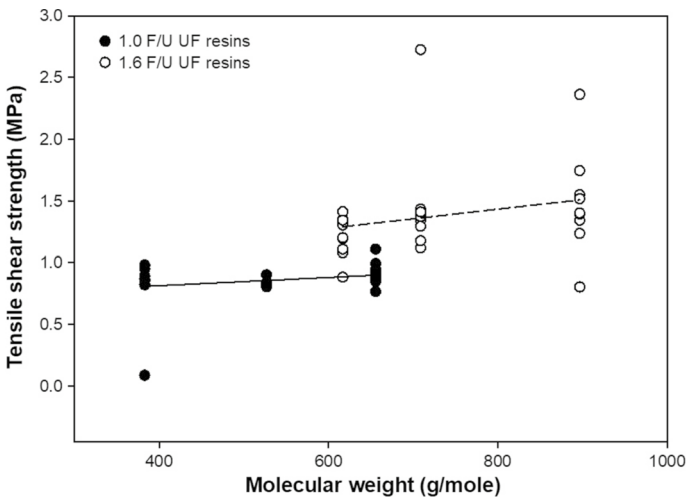
Fig. 16 TSS of plywood bonded with 1.0 and 1.6 UF resins with L-MW, M-MW, and H-MW. *The statistical data related to this figure are presented in the supplementary information (Table S2)

Conclusion

This study attempted to understand the influence of MW on the wettability, surface adhesion, interphase adhesion, and adhesion strength in wood bonding using UF resins at two molar ratios, different types of wood (earlywood, latewood, sapwood, and heartwood) before and after the extractive removal. As the molar ratio increases, the viscosity and MW of UF resins increase. As the MW increases, the surface tension of 1.0 UF resins slightly increases, whereas that of 1.6 UF resins decreases even though the surface tension of the former is greater than that of the latter. Regardless of the MW of UF resins, the contact angle and maximum surface adhesion force are smaller on the earlywood surface with higher roughness values than those on the latewood surface. The contact angle shows a weak negative correlation with the surface roughness of wood, leading to a decrease in the maximum surface adhesion force. The wettability and surface adhesion force of UF resins with different MWs on wood surface did not proportionately improve their adhesion in interphase and plywood. These results suggest that the MW, wettability, and surface adhesion are indirectly related to interphase adhesion and cohesion in wood bonding, and the surface roughness is a dominant factor for the wettability and surface adhesion force.

Declarations

Conflict of interest The authors have no competing interests to declare.

References

Alade AA, Naghizadeh Z, Wessels CB, Tyhoda L (2022) A review of the effects of wood preservative impregnation on adhesive bonding and joint performance. J Adhes Sci Technol 36(15):1593–1617. https://doi.org/10.1080/01694243.2021.1981651

Alam N, Islam N, Rahman K-S, Alam MR (2012) Comparative study on physical and mechanical properties of plywood produced from eucalyptus (Eucalyptus camaldulensis Dehn.) and simul (Bombax ceiba L.) veneers. Res J Recent Sci 1(9):54–58

Amorim MRS, Ribeiro PG, Martins SA et al (2013) Surface wettability and roughness of 11 amazonian tropical hardwoods. Floresta Ambient 20:99–109. https://doi.org/10.4322/floram.2012.069

Baier RE, Shafrin EG, Zisman WA (1968) Adhesion: Mechanisms that assist or impede it. Science 162:1360–1368. https://doi.org/10.1126/science.162.3860.1360

Belt T, Keplinger T, Hänninen T, Rautkari L (2017) Cellular level distributions of Scots pine heartwood and knot heartwood extractives revealed by Raman spectroscopy imaging. Ind Crops Prod 108:327–335. https://doi.org/10.1016/j.indcrop.2017.06.056

Belt T, Venäläinen M, Altgen M et al (2021) Extractive concentrations and cellular-level distributions change radially from outer to inner heartwood in Scots pine. Tree Physiol 41:1034–1045. https://doi.org/10.1093/treephys/tpaa166

Berg JC (1993) The importance of acid-base interactions in wetting, coating, adhesion and related phenomena. Nord Pulp Pap Res J 8(1):75–85. https://doi.org/10.3183/npprj-1993-08-01-p075-085

Bergström B, Gustafsson G, Gref R, Ericsson A (1999) Seasonal changes of pinosylvin distribution in the sapwood/heartwood boundary of Pinus sylvestris. Trees Struct Funct 14:65–71. https://doi.org/10.1007/s004680050210

Butt HJ, Roisman IV, Brinkmann M et al (2014) Characterization of super liquid-repellent surfaces. Curr Opin Colloid Interface Sci 19:343–354. https://doi.org/10.1016/j.cocis.2014.04.009

Celedon JM, Bohlmann J (2018) An extended model of heartwood secondary metabolism informed by functional genomics. Tree Physiol 38(3):311–319. https://doi.org/10.1093/treephys/tpx070

Chen CM (1970) Effect of extractive removal on adhesion and wettability of some tropical woods. For Prod J 20:36–41. https://doi.org/10.5658/WOOD.2019.47.5.579

Chen H, Tang T, Amirfazli A (2015) Effects of surface wettability on fast liquid transfer. Phys Fluids 27:1–15. https://doi.org/10.1063/1.4934961

Chen H, Tang T, Zhao H et al (2016) How pinning and contact angle hysteresis govern quasi-static liquid drop transfer. Soft Matter 12:1998–2008. https://doi.org/10.1039/c5sm02451j

Cheng E, Sun X (2006) Effects of wood-surface roughness, adhesive viscosity and processing pressure on adhesion strength of protein adhesive. J Adhes Sci Technol 20(9):997–1017. https://doi.org/10.1163/156856106777657779

Cherelli SG, Sartori MMP, Próspero AG, Ballarin AW (2018) Heartwood and sapwood in eucalyptus trees: Non-conventional approach to wood quality. Acad Bras Cienc 90:425–438. https://doi.org/10.1590/0001-3765201820160195

Collett BM (1972) A review of surface and interfacial adhesion in wood science and related fields. Wood Sci Technol 6:1–42. https://doi.org/10.1007/BF00351806

Dehon L, Macheix JJ, Durand M (2002) Involvement of peroxidases in the formation of the brown coloration of heartwood in Juglans nigra. J Exp Bot 53(367):303–311. https://doi.org/10.1093/jexbot/53.367.303

DIN 53914 (1997) Determination of the surface tension. Berlin, Germany

Dunky M (1998) Urea–formaldehyde (UF) adhesive resins for wood. In.t. J Adhes Adhes 18:95–107

Follrich J, Vay O, Veigel S, Müller U (2010) Bond strength of end-grain joints and its dependence on surface roughness and adhesive spread. J Wood Sci 56(5):429–434. https://doi.org/10.1007/s10086-010-1118-1

Freeman HA (1959) Relation between physical and chemical properties of wood and adhesion. For Prod J 9(12):451–458

Gao Z, Wang XM, Wan H, Liu Y (2008) Curing characteristics of urea-formaldehyde resin in the presence of various amounts of wood extracts and catalysts. J Appl Polym Sci 107(3):1555–1562. https://doi.org/10.1002/app.27205

Gavrilovíc-Grmuša I, Miljković J, Diporovíc-Momčilovíč M (2010) Influence of the degree of condensation on the radial penetration of urea-formaldehyde adhesives into silver fir (Abies alba, Mill.) wood tissue. J Adhes Sci Technol 24:1437–1453. https://doi.org/10.1163/016942410X501034

Gavrilović-Grmuša I, Dunky M, Miljković J, Djiporović-Momčilović M (2010) Radial penetration of urea-formaldehyde adhesive resins into beech (Fagus moesiaca). J Adhes Sci Technol 24:1753–1768. https://doi.org/10.1163/016942410X507812

Gavrilovic-Grmusa I, Dunky M, Miljkovic J, Djiporovic-Momcilovic M (2012) Influence of the viscosity of UF resins on the radial and tangential penetration into poplar wood and on the shear strength of adhesive joints. Holzforschung 66:849–856. https://doi.org/10.1515/hf-2011-0177

Ghofrani M, Mirkhandouzi FZ, Ashori A (2016) Effects of extractives removal on the performance of clear varnish coatings on boards. J Compos Mater 30(21):3019–3024. https://doi.org/10.1177/0021998315615205

Henry C, Minier JP, Lefèvre G (2012) Numerical study on the adhesion and reentrainment of nondeformable particles on surfaces: The role of surface roughness and electrostatic forces. Langmuir 28(1):438–452. https://doi.org/10.1021/la203659q

Hillis WE (1962) Wood extractives and their significance to the pulp and paper industries. Academic Press, USA

Hillis WE (1972) Formation and properties of some wood extractives. Phytochem 11(47):1207–1218

Hong MK, Park BD (2017) Effect of urea-formaldehyde resin adhesive viscosity on plywood adhesion. J Korean Wood Sci Technol 45:223–231. https://doi.org/10.5658/WOOD.2017.45.2.223

Hse CY (1972a) Method for computing a roughness factor for veneer surfaces. Wood Sci 4:229–232

Hse CY (1972b) Wettability of southern pine veneer by phenol formaldehyde wood adhesives. For Prod J 22:51–56

Hse CY, Kuo M (1988) Influence of extractives on wood gluing and finishing - a review. For Prod J 38:52–56

ISO 4288 (1997) Surface texture: profile method - rules and procedures for the assessment of surface texture. Berlin, Germany

Jeong B, Park BD (2017) Effect of analytical parameters of gel permeation chromatography on molecular weight measurements of urea-formaldehyde resins. J Korean Wood Sci Technol 45:471–481. https://doi.org/10.5658/WOOD.2017.45.4.471

Jeong B, Park BD (2019a) Performance of urea-formaldehyde resins synthesized at two different low molar ratios with different numbers of urea addition. J Korean Wood Sci Technol 47:221–228. https://doi.org/10.5658/WOOD.2019.47.2.221

Jeong B, Park BD (2019b) Effect of molecular weight of urea–formaldehyde resins on their cure kinetics, interphase, penetration into wood, and adhesion in bonding wood. Wood Sci Technol 53:665–685. https://doi.org/10.1007/s00226-019-01092-1

Jiang S, Hu M, Du G et al (2021) Highly branched polyurea-enhanced urea-formaldehyde resin. ACS Appl Polym Mater 3:1157–1170. https://doi.org/10.1021/acsapm.0c01362

Joe J, Thouless MD, Barber JR (2020) Effect of surface roughness on adhesive instabilities for the elastic layer. Front Mech Eng. https://doi.org/10.3389/fmech.2020.00031

Kamke FA, Lee JN (2007) Adhesive penetration in wood - a review. Wood Fiber Sci 39:205–220

Khan S, Chui YH, Schneider MH, Barry AO (2004) Wettability of treated flakes of selected species with commercial adhesive resins. J Institute of Wood Sci 16(5):238–263

KS F 3101 (2020) Plywood, Korea Standard Association, Seoul, Korea

Laborie MPG, Salmén L, Frazier CE (2006) A morphological study of the wood/phenol-formaldehyde adhesive interphase. J Adhes Sci Technol 20:729–741. https://doi.org/10.1163/156856106777638743

Lee S, Shupe TF, Groom LH, Hse CY (2007) Wetting behaviors of phenol - and urea-formaldehyde resins as compatibilizers. Wood Fiber Sci 38:482–492

Li J, Zhang Y (2021) Morphology and crystallinity of urea-formaldehyde resin adhesives with different molar ratios. Polym (basel) 13(5):673. https://doi.org/10.3390/polym13050673

Liang J, Li T, Cao M, Du G (2018) Urea-formaldehyde resin structure formation under alkaline condition: a quantitative 13C-NMR study. J Adhes Sci Technol 32:439–447. https://doi.org/10.1080/01694243.2017.1361127

Lloyd JA (1978) Distribution of extractives in Pinus radiata earlywood and latewood. New Zeal J for Sci 8(2):288–294

Lubis MAR, Park BD (2018) Modification of urea-formaldehyde resin adhesives with oxidized starch using blocked pMDI for plywood. J Adhes Sci Technol 32(24):2667–2681. https://doi.org/10.1080/01694243.2018.1511075

Lubis MAR, Park BD (2020) Influence of initial molar ratios on the performance of low molar ratio urea-formaldehyde resin adhesives. J Korean Wood Sci Technol 48:136–153. https://doi.org/10.5658/WOOD.2020.48.2.136

Lubis MAR, Park BD (2021) Enhancing the performance of low molar ratio urea–formaldehyde resin adhesives via in-situ modification with intercalated nanoclay. J Adhes 97:1271–1290. https://doi.org/10.1080/00218464.2020.1753515

Matsushita Y, Jang IC, Imai T et al (2012) Distribution of extracts including 4,8-dihydroxy-5-methoxy-2-naphthaldehyde in Diospyros kaki analyzed by gas chromatography-mass spectrometry and time-of-flight secondary ion mass spectrometry. Holzforschung 66:705–709. https://doi.org/10.1515/hf-2011-0214

Matuana LM, Balatinecz JJ, Park CB (1998) Between PVC and wood veneer laminates. Polym Eng Sci 3:765–773

Merela M, Čufar K (2013) Gustoća i mehanička svojstva drva bjeljike hrasta u usporedbi s drvom srži. Drv Ind 64:323–334. https://doi.org/10.5552/drind.2013.1325

Metsä-Kortelainen S, Viitanen H (2012) Wettability of sapwood and heartwood of thermally modified Norway spruce and Scots pine. Eur J Wood Prod 70(1):135–139. https://doi.org/10.1007/s00107-011-0523-5

Myers GE (1984) How mole ratio of uf resin affects formaldehyde emission and other properties: a literature critiquE. For Prod J 34(5):35–41

Myers D (1999) Surfaces, Interfaces, and Colloids: Principles and Applications, Wiley-VCH, 2nd Edition. London, UK

Nayar KG, Panchanathan D, McKinley GH, Lienhard JH (2014) Surface tension of seawater. J Phys Chem Ref Data 43(4):04313. https://doi.org/10.1063/1.4899037

Nuryawan A, Park BD, Singh AP (2014) Penetration of urea-formaldehyde resins with different formaldehyde/urea mole ratios into softwood tissues. Wood Sci Technol 48:889–902. https://doi.org/10.1007/s00226-014-0649-9

Nuryawan A, Singh AP, Zanetti M et al (2017) Insights into the development of crystallinity in liquid urea-formaldehyde resins. Int J Adhes Adhes 72:62–69. https://doi.org/10.1016/j.ijadhadh.2016.10.004

Nussbaum RM, Sterley M (2002) The effect of wood extractive content on glue adhesion and surface wettability of wood. Wood Fiber Sci 34:57–71

Pang S, Herritsch A (2005) Physical properties of earlywood and latewood of Pinus radiata D. Don: anisotropic shrinkage, equilibrium moisture content and fibre saturation point. Holzforschung 59:654–661. https://doi.org/10.1515/HF.2005.105

Papp EA, Csiha C (2017) Contact angle as function of surface roughness of different wood species. Surf and Interfaces 8:54–59. https://doi.org/10.1016/j.surfin.2017.04.009

Park B-D (2007) Properties of urea-formaldehyde resin adhesives with different formaldehyde to urea mole ratios. J Korean Wood Sci Technol 35(5):67–75

Park BD, Kang EC, Park JY (2006) Effects of formaldehyde to urea mole ratio on thermal curing behavior of urea-formaldehyde resin and properties of particleboard. J Appl Polym Sci 101(3):1787–1792. https://doi.org/10.1002/app.23538

Patton TC (1970) A simplified review of adhesion theory based on surface energetics. TAPPI 53(3):421. https://doi.org/10.1002/app.22608

Petrič M, Oven P (2015) Determination of wettability of wood and its significance in wood science and technology: a critical review. Rev Adhes Adhes 3(2):121–187

Pizzi A (1983) Wood adhesives chemistry and technology, Vol. 1, Marce-Dekker, New York, USA

Pizzi A, Mittal K, Pizzi A (2003) Urea–Formaldehyde Adhesives. Handbook of Adhes Technol. Marce-Dekker, New York, USA. Doi: https://doi.org/10.1201/9780203912225.ch31

Plomion C, Leprovost G, Stokes A (2001) Wood formation in trees. Plant Physiol 127(4):1513–1523

Que Z, Furuno T, Katoh S, Nishino Y (2007) Effects of urea-formaldehyde resin mole ratio on the properties of particleboard. Build Environ 42(3):1257–1263. https://doi.org/10.1016/j.buildenv.2005.11.028

Rapp BE (2017) Measuring surface tension and free surface energy. Microfluid Model Mech Math. https://doi.org/10.1016/b978-1-4557-3141-1.50022-8

Rathke J, Sinn G (2013) Evaluating the wettability of MUF resins and pMDI on two different OSB raw materials. Eur J Wood Prod 71:335–342. https://doi.org/10.1007/s00107-013-0675-6

Rezaee Niaraki P, Krause A (2020) Correlation between physical bonding and mechanical properties of wood plastic composites: Part 1: interaction of chemical and mechanical treatments on physical properties. J Adhes Sci Technol 34:744–755. https://doi.org/10.1080/01694243.2019.1683325

Roffael E (2016) Significance of wood extractives for wood bonding. Appl Microbiol Biotechnol 100:1589–1596. https://doi.org/10.1007/s00253-015-7207-8

Santoni I, Pizzo B (2011) Effect of surface conditions related to machining and air exposure on wettability of different Mediterranean wood species. Int J Adhes Adhes 31(7):743–753. https://doi.org/10.1016/j.ijadhadh.2011.07.002

Santoso M, Widyorini R, Prayitno TA et al (2019) The effects of extractives substances for bonding performance of three natural binder on nipa fronds particleboard. KnE Life Sci. https://doi.org/10.18502/kls.v4i11.3868

Scheikl M, Dunky M (1998) Measurement of dynamic and static contact angles on wood for the determination of its surface tension and the penetration of liquids into the wood surface. Holzforschung 52:89–94

Šernek M, Kamke FA, Glasser WG (2004) Comparative analysis of inactivated wood surface. Holzforschung 58:22–31. https://doi.org/10.1515/HF.2004.004

Shi SQ, Gardner DJ (2001) Dynamic adhesive wettability of wood. Wood Fiber Sci 33:58–68

Shin PS, Baek YM, Kim JH et al (2018) Interfacial and wetting properties between glass fiber and epoxy resins with different pot lives. Colloids Surf A Physicochem Eng Asp 544:68–77. https://doi.org/10.1016/j.colsurfa.2018.02.017

Shupe TE, Hse CY, Choong ET, Groom LH (1998) Effect of wood grain and veneer side on loblolly pine veneer wettability. For Prod J 48(6):95–97

Shupe TF, Hse CY, Wang WH (2001) An investigation of selected factors that influence hardwood wettability. Holzforschung 55:541–548. https://doi.org/10.1515/HF.2001.087

Siimer K, Kaljuvee T, Christjanson P (2003) Thermal behaviour of urea-formaldehyde resins during curing. J Therm Anal Calorim 72:607–617. https://doi.org/10.1023/A:1024590019244

Singleton R, DeBell DS, Gartner BL (2003) Effect of extraction on wood density of western hemlock (Tsuga heterophylla (Raf.) Sarg.). Wood Fiber Sci 35:363–369

Sinn G, Gindl M, Reiterer A, Stanzl-Tschegg S (2004) Changes in the surface properties of wood due to sanding. Holzforschung 58:246–251. https://doi.org/10.1515/HF.2004.038

Steinhof O, Kibrik ÉJ, Scherr G, Hasse H (2014) Quantitative and qualitative 1H, 13C, and 15N NMR spectroscopic investigation of the urea-formaldehyde resin synthesis. Magn Reson Chem 52:138–162. https://doi.org/10.1002/mrc.4044

Sun Y, Jiang Y, Choi CH et al (2017) Direct measurements of adhesion forces of water droplets on smooth and patterned polymers. Surf Innov 6:93–105. https://doi.org/10.1680/jsuin.17.00049

T 204-cm-97 (1997) Solvent extractives of wood and pulp, TAPPI, Atlanta, USA

Timell TE (1986) Compression wood in gymnosperms, vol 1. Springer-Verlag, Berlin, Germany

van Oss CJ (1993) A review of wettability. In: Berg JC (ed) Marcel Dekker, New York

Vaziri M, Karlsson O, Abrahamsson L (2021) Wettability of welded wood-joints investigated by the Wilhelmy method: Part 1. Determination of apparent contact angles, swelling, and water sorption. Holzforschung 75:65–74. https://doi.org/10.1515/hf-2019-0308

Wålinder MEP, Ström G (2001) Measurement of wood wettability by the wilhelmy method. Holzforschung 55:33–41. https://doi.org/10.1515/hfsg.2001.33

Walinder M (2000) Wettability Phenomena on Wood: Factors Influencing Measurements Of Wood Wettability. Dr Thesis, Dept. Manuf. Syst. Wood Technol. Process, KTH-Royal Inst Technol, Stockholm, Sweden

Wang ZJ, Kwon DJ, Lawrence DeVries K, Park JM (2015) Frost formation and anti-icing performance of a hydrophobic coating on aluminum. Exp Therm Fluid Sci 60:132–137. https://doi.org/10.1016/j.expthermflusci.2014.09.003

Wang H, Cao M, Li T et al (2018) Characterization of the low molar ratio urea-formaldehyde resin with 13C NMR and ESI-MS: Negative effects of the post-added urea on the urea-formaldehyde polymers. Polym (basel) 10(6):602. https://doi.org/10.3390/polym10060602

Wang D, Jiang Y, Zhu Z et al (2020) Contact line and adhesion force of droplets on concentric ring-textured hydrophobic surfaces. Langmuir 36(10):2622–2628. https://doi.org/10.1021/acs.langmuir.9b03953

Whitesides GM, Biebuyck HA, Folkers JP, Prime KL (1991) Acid-base interactions in wetting. J Adhes Sci Technol 5:57–69. https://doi.org/10.1163/156856191X00828

Wibowo ES, Park BD (2021a) Crystalline lamellar structure of thermosetting urea-formaldehyde resins at a low molar ratio. Macromolecules 54(5):2366–2375. https://doi.org/10.1021/acs.macromol.1c00073

Wibowo ES, Park BD (2021b) Direct measurement of surface adhesion between thin films of nanocellulose and urea–formaldehyde resin adhesives. Cellulose 28:8459–8481. https://doi.org/10.1007/s10570-021-04088-y

Wibowo ES, Park BD (2022) Two-dimensional nuclear magnetic resonance analysis of hydrogen-bond formation in thermosetting crystalline urea-formaldehyde resins at a low molar ratio. ACS Appl Polym Mater 4:1084–1094. https://doi.org/10.1021/acsapm.1c01521

Wibowo ES, Lubis MAR, Park BD (2020a) Converting crystalline thermosetting urea–formaldehyde resins to amorphous polymer using modified nanoclay. J Ind Eng Chem 87:78–89. https://doi.org/10.1016/j.jiec.2020.03.014

Wibowo ES, Park BD, Causin V (2020b) Hydrogen-bond-induced crystallization in low-molar-ratio urea-formaldehyde resins during synthesis. Ind Eng Chem Res 59:13095–13104. https://doi.org/10.1021/acs.iecr.0c02268

Wilkes J (1984) The influence of rate of growth on the density and heartwood extractives content of eucalypt species. Wood Sci Technol 18(2):113–120. https://doi.org/10.1007/BF00350470

Xu HN, Shen QY, Ouyang XK, Yang LY (2012) Wetting of soy protein adhesives modified by urea on wood surfaces. Eur J Wood Prod 70:11–16. https://doi.org/10.1007/s00107-010-0502-2

Yang Z, Peng H, Wang W, Liu T (2010) Crystallization behavior of poly(ε-caprolactone)/layered double hydroxide nanocomposites. J Appl Polym Sci 116:2658–2667. https://doi.org/10.1002/app

Yin J, Song K, Lu Y et al (2015) Comparison of changes in micropores and mesopores in the wood cell walls of sapwood and heartwood. Wood Sci Technol 49(5):987–1001. https://doi.org/10.1007/s00226-015-0741-9

Zhang C, Fujita M, Takabe K (2004) Extracellular diffusion pathway for heartwood substances in Albizia julibrissin Durazz. Holzforschung 58:495–500. https://doi.org/10.1515/HF.2004.075